

LETTER TO THE EDITOR

Optical circular polarization in quasars^{★,★★}

D. Hutsemékers^{1,★★}, B. Borguet², D. Sluse³, R. Cabanac⁴, and H. Lamy⁵

¹ Institut d’Astrophysique et de Géophysique, Université de Liège, Allée du 6 Août 17, B5c, 4000 Liège, Belgium
e-mail: hutsemekers@astro.ulg.ac.be

² Department of Physics, Virginia Polytechnic and State University, Blacksburg, VA 24061, USA

³ Zentrum für Astronomie der Universität Heidelberg, Mönchhofstr. 12-14, 69120 Heidelberg, Germany

⁴ Laboratoire d’Astrophysique de Toulouse-Tarbes, Université de Toulouse, 57 avenue d’Azereix, 65000 Tarbes, France

⁵ Institut Belge d’Aéronomie Spatiale, Avenue Circulaire 3, 1180 Bruxelles, Belgium

Received 7 July 2010 / Accepted 19 September 2010

ABSTRACT

We present new optical circular polarization measurements with typical uncertainties $<0.1\%$ for a sample of 21 quasars. All but two objects have null circular polarization. We use this result to constrain the polarization due to photon-pseudoscalar mixing along the line of sight. We detect significant ($>3\sigma$) circular polarization in two blazars with high linear polarization and discuss the implications of this result for quasar physics. In particular, the recorded polarization degrees may be indicative of magnetic fields as strong as 1 kG or a significant contribution of inverse Compton scattering to the optical continuum.

Key words. quasars: general – polarization

1. Introduction

To interpret the large-scale alignments of quasar optical polarization vectors observed at redshifts $z \sim 1$ (Hutsemékers 1998; Hutsemékers & Lamy 2001; Hutsemékers et al. 2005) polarization induced by photon-pseudoscalar mixing along the line of sight has been invoked (Hutsemékers 1998; Jain et al. 2002). Photon-pseudoscalar mixing generates dichroism and birefringence, the latter transforming linear polarization into circular polarization and vice-versa along the line of sight. If photon-pseudoscalar mixing produces the linear polarization needed to explain the observed alignments, a comparable amount of circular polarization would be expected (Raffelt & Stodolsky 1988; Jain et al. 2002; Das et al. 2005; Gnedin et al. 2007; Hutsemékers et al. 2008; Payez et al. 2008). Hence, we present accurate circular polarization measurements for a sample of quasars whose polarization vectors are coherently oriented.

The optical circular polarization of quasars has rarely been measured. Our new observations, data reduction, and a compilation of published measurements are presented in Sect. 2. Implications for the photon-pseudoscalar mixing mechanism are discussed in Sect. 3.1. The detection of significant circular polarization in two objects and its consequence for quasar physics are presented in Sect. 3.2.

2. Observations and data reduction

The observations were carried out on April 18–20, 2007 at the European Southern Observatory (ESO, La Silla) using the 3.6 m

telescope equipped with the ESO Faint Object Spectrograph and Camera EFOSC2. Circular polarization was measured using a super-achromatic quarter-wave ($\lambda/4$) retarder plate (QWP), which transforms the circular polarization into linear polarization, and a Wollaston prism, which splits the linearly polarized beam into two orthogonally polarized images of the object (Saviane et al. 2007). The CCD was used in unbinned mode, which corresponds to a scale of $0.157''/\text{pixel}$ on the sky. All measurements were performed through a Bessel *V* filter (V#641; central wavelength: 5476 Å; *FWHM*: 1132 Å).

At least one pair of exposures with the QWP rotated to the angles -45° and $+45^\circ$ was secured for each target. Frames were dark-subtracted and flat-fielded. The circular polarization p_0 , i.e., the normalized Stokes V/I parameter, was extracted from each pair of frames using a procedure used to measure the normalized Stokes Q/I and U/I parameters and described in Lamy & Hutsemékers (1999) and Sluse et al. (2005). Errors were estimated from the photon noise. Seeing was typically around $1''$. Owing to the variable atmospheric extinction (thin to thick cirrus), some exposures had to be repeated to reach a sufficient signal-to-noise ratio.

The performances of the instrument were checked during our run and during the setup night (April 17) using an unpolarized standard star and a star with high and slowly variable circular polarization, LP 790–20 (West 1989; Jordan & Friedrich 2002). The results, discussed in Saviane et al. (2007), demonstrated the quality of the instrumental setup. LP 790–20 was also used to fix the sign of the circular polarization, i.e., $p_{\text{circ}} > 0$ when the electric vector rotates counter-clockwise as seen by an observer facing the object.

To evaluate the cross-talk between linear and circular polarization, we measured the circular polarization of linearly polarized stars. These observations were repeated several times during our observing run. Hilt 652 was observed during the setup

[★] Based on observations made with ESO Telescopes at the La Silla Observatory (Chile). ESO program ID: 79.A-0625(B).

^{★★} Appendices are only available in electronic form at
<http://www.aanda.org>

^{***} Maître de Recherches au F.R.S.-FNRS.

Table 1. The circular polarization of linearly polarized standard stars.

Object	$p_{\text{lin}} (\%)$	$\theta_{\text{lin}} (\circ)$	$p_{\text{circ}} (\%)$
Hilt 652	6.25 ± 0.03	179.2 ± 0.2^a	0.003 ± 0.021
Ve 6–23	8.26 ± 0.05	171.6 ± 0.2^a	-0.050 ± 0.035
HD155197	4.38 ± 0.03	103.2 ± 0.2^b	0.033 ± 0.025

Notes. All these polarization measurements were obtained in the V filter. References for linear polarization: ^(a) Fossati et al. (2007); ^(b) Turnshek et al. (1990).

Table 2. New circular polarization measurements of quasars.

Object	z	$p_{\text{lin}} (\%)$	$\theta_{\text{lin}} (\circ)$	$p_{\text{circ}} (\%)$
1120+019	1.465	1.95 ± 0.27	9 ± 4^c	-0.02 ± 0.05
1124–186	1.048	11.68 ± 0.36	37 ± 1^g	-0.04 ± 0.08
1127–145	1.187	1.30 ± 0.40 [w]	23 ± 10^a	-0.05 ± 0.05
1157+014	1.990	0.76 ± 0.18	39 ± 7^f	-0.10 ± 0.08
1205+146	1.640	0.83 ± 0.18	161 ± 6^f	-0.10 ± 0.09
1212+147	1.621	1.45 ± 0.30	24 ± 6^c	0.15 ± 0.09
1215–002*	0.420	23.94 ± 0.70	91 ± 1^g	-0.42 ± 0.40
1216–010	0.415	11.20 ± 0.17	100 ± 1^g	-0.01 ± 0.07
1222+228	2.058	0.92 ± 0.14	169 ± 4^g	0.01 ± 0.10
1244–255	0.633	8.40 ± 0.20 [w]	110 ± 1^a	-0.23 ± 0.20
1246–057	2.236	1.96 ± 0.18 [w]	149 ± 3^e	0.01 ± 0.03
1254+047	1.024	1.22 ± 0.15 [w]	165 ± 3^b	-0.02 ± 0.04
1256–229*	0.481	22.32 ± 0.15	157 ± 1^g	0.18 ± 0.04
1309–056	2.212	0.78 ± 0.28	179 ± 11^c	-0.08 ± 0.06
1331–011	1.867	1.88 ± 0.31	29 ± 5^c	-0.04 ± 0.06
1339–180	2.210	0.83 ± 0.15	20 ± 5^g	-0.01 ± 0.07
1416–129	0.129	1.63 ± 0.15 [w]	44 ± 3^b	0.05 ± 0.06
1429–008	2.084	1.00 ± 0.29	9 ± 9^c	0.02 ± 0.08
2121+050	1.878	10.70 ± 2.90 [w]	68 ± 6^a	0.02 ± 0.15
2128–123	0.501	1.90 ± 0.40 [w]	64 ± 6^d	-0.04 ± 0.03
2155–152	0.672	22.60 ± 1.10 [w]	7 ± 2^a	-0.35 ± 0.10

Notes. Linear and circular polarizations were measured in the V filter except a series of linear polarization data from the literature measured in white light and noted [w]; ^(*) 1215–002 is classified as a BL Lac by Collinge et al. (2005); Sbarufatti et al. (2005) re-determined the redshift of 1256–229 ($z = 0.481$) and considered this object as a BL Lac. References for linear polarization: ^(a) Impey & Tapia (1990); ^(b) Berriman et al. (1990); ^(c) Hutsemékers et al. (1998); ^(d) Visvanathan & Wills (1998); ^(e) Schmidt & Hines (1999); ^(f) Lamy & Hutsemékers (2000); ^(g) Sluse et al. (2005).

night. The results are given in Table 1 together with the published linear polarization (i.e. the polarization degree p_{lin} and the polarization position angle θ_{lin}). Uncertainties are smaller than in Saviane et al. (2007) because of the availability of repeated observations. Although the objects are highly linearly polarized, we measure a null circular polarization. Combining the data of Hilt 652 and Ve 6–23, which have similar polarization angles, we derive the 3σ upper limit to the circular polarization due to cross-talk in the V filter $|p_{\text{circ}}/p_{\text{lin}}| \lesssim 0.0075$.

Our new measurements of quasar circular polarization are reported in Table 2 with 1σ photon-noise errors. The targets are extracted from the sample of 355 polarized quasars defined in Hutsemékers et al. (2005), as well as their B1950 names/coordinates, their redshift z , and their linear polarization degree and angle, p_{lin} and θ_{lin} .

A compilation of other measurements of quasar optical circular polarization is given in Table 3. Unless indicated otherwise, these measurements were obtained in white light, i.e., in the 3200–8800 Å or 4000–8800 Å spectral ranges, which

Table 3. Previous circular polarization measurements of quasars and BL Lac objects.

Object	z	$p_{\text{lin}} (\%)$	$\theta_{\text{lin}} (\circ)$	$p_{\text{circ}} (\%)$
0237–233	2.223	0.25 ± 0.29	– ^d	-0.06 ± 0.08^a
0955+326	0.533	0.18 ± 0.24	– ^c	0.06 ± 0.08^a
1127–145	1.187	1.30 ± 0.40	23 ± 10^e	0.32 ± 0.20^a
1156+295	0.729	2.68 ± 0.41	114 ± 4^f	0.12 ± 0.14^b
1222+228	2.058	1.09 ± 0.16 [u]	167 ± 4^i	0.23 ± 1.80^i
1226+023	0.158	0.25 ± 0.04	58 ± 4^c	-0.01 ± 0.02^g
1253–055	0.536	9.00 ± 0.40	67 ± 1^e	0.09 ± 0.07^a
1308+326	0.997	12.10 ± 1.50	68 ± 3^e	-0.08 ± 0.17^b
1634+706	1.334	0.24 ± 0.07 [u]	4 ± 8^i	-0.05 ± 0.09^i
1641+399	0.594	4.00 ± 0.30	103 ± 2^e	-0.05 ± 0.23^b
2230+114	1.037	7.30 ± 0.30	118 ± 1^e	-0.05 ± 0.17^a
2302+029	1.044	0.66 ± 0.12 [u]	136 ± 5^i	-0.39 ± 0.16^i
0138–097	0.733	3.60 ± 1.50	168 ± 11^e	0.25 ± 0.35^k
0219+428	0.444	26.11 ± 0.19	3 ± 1^k	0.16 ± 0.05^k
0422+004	0.310	10.29 ± 0.23	179 ± 1^g	0.14 ± 0.07^g
0735+178	0.424	11.69 ± 0.22	123 ± 1^k	0.03 ± 0.05^k
0823–223	0.910	14.39 ± 0.16	11 ± 1^k	0.16 ± 0.08^k
0851+202	0.306	10.80 ± 0.30	156 ± 1^e	-0.01 ± 0.02^a
1101+384	0.031	2.59 ± 0.11	10 ± 1^h	0.02 ± 0.03^h
2155–304	0.116	4.12 ± 0.25	93 ± 2^j	-0.02 ± 0.02^j
2200+420	0.068	4.90 ± 0.40	147 ± 2^e	-0.07 ± 0.19^a

Notes. All but a few polarization measurements were obtained in white light; the multi-color measurements in references (h), (j) and (k) were averaged; [u] refers to linear and circular polarization measurements averaged over the 2200–3200 Å ultraviolet wavelength band; the circular polarization of objects 2200+420 and 2230+114 was obtained in the 4000–6000 Å and 3500–5200 Å bands respectively; italicized names indicate objects classified as BL Lac in Véron-Cetty & Véron (2006). References for linear and circular polarization: ^(a) Landstreet & Angel (1972); ^(b) Moore & Stockman (1981); ^(c) Stockman et al. (1984); ^(d) Moore & Stockman (1984); ^(e) Impey & Tapia (1990); ^(f) Wills et al. (1992); ^(g) Valtaoja et al. (1993); ^(h) Takalo & Sillanpää (1993); ⁽ⁱ⁾ Impey et al. (1995); ^(j) Tommasi et al. (2001a); ^(k) Tommasi et al. (2001b).

roughly correspond to an effective wavelength of 6000 Å. When several estimates of either linear or circular polarization are available, only the value with the smallest uncertainty is considered. BL Lac objects, similar in many respects to highly polarized quasars (HPQs) (e.g., Scarpa & Falomo 1997; Fan et al. 2008), are included. Both BL Lac and HPQs belong to the blazar sub-group of active galactic nuclei (AGN). For BL Lac objects, the polarization is often strongly variable. We then adopt the circular polarization with the smallest uncertainty and, when quasi-simultaneous observations are available, the value of the linear polarization obtained as close as possible in time. Otherwise we select a representative value of the linear polarization from the survey of Impey & Tapia (1990).

3. Discussion

The measurements reported in Tables 2 and 3 show that all quasars and BL Lac objects have null circular polarization ($<3\sigma$) except two HPQs, 1256–229 and 2155–152, and one highly polarized BL Lac object, 0219+428.

We first discuss the constraints provided by the majority of null detections on the photon-pseudoscalar mixing mechanism, and then the consequences of the three detections for blazar physics.

3.1. Constraints on photon-pseudoscalar mixing

Quasars with right ascension between $11^{\text{h}}20^{\text{m}}$ and $14^{\text{h}}30^{\text{m}}$ belong to the region of alignment A1 defined in Hutsemékers (1998). In this region of the sky, quasars with $1 < z < 2.3$ have their polarization angle preferentially in the range $[146^{\circ}–226^{\circ}]$ (modulo 180°), while quasars with $0 < z < 1$ have their polarization angle preferentially in the range $[30^{\circ}–120^{\circ}]$. Assuming that the quasar intrinsic polarization vectors are randomly oriented, the addition of a small systematic linear polarization $\Delta p_{\text{lin}} \simeq 0.5\%$ at a fixed position angle can account for the observed alignments (Hutsemékers et al. 2008, Appendix A). If photon-pseudoscalar mixing is responsible for this extra linear polarization, one expects, on average, that $|p_{\text{circ}}| \simeq \Delta p_{\text{lin}} \simeq 0.5\%$ (Appendix B). Because the light from most quasars is intrinsically linearly polarized to some extent and not circularly polarized, limits on any additional polarization from interactions along the line of sight cannot be derived from the measurement of the linear polarization degree, while, on the other hand, useful constraints can be derived from the measurement of circular polarization.

Most of the thirteen quasars with $z > 1$ located in region A1 were found to have $|p_{\text{circ}}| \lesssim 0.25\%$ (3σ upper limit), which is definitely smaller than the expected value. Averaging over the thirteen objects, we infer that $\langle |p_{\text{circ}}| \rangle = 0.035 \pm 0.016\%$ after neglecting the sign, from which a stringent 3σ upper limit on the circular polarization of $\langle |p_{\text{circ}}| \rangle \leq 0.05\%$ can be derived. This limit is one order of magnitude smaller than the expected value $|p_{\text{circ}}| \simeq 0.5\%$. A similar result is obtained for the nine objects at $z < 1$ in that region.

This result rules out the interpretation of the observed alignments in terms of photon-pseudoscalar mixing, at least in its simplest formulation. A more complex treatment of the photon-pseudoscalar interaction is thus required to account for the observations (Payez et al. 2010a,b).

3.2. Detection of optical circular polarization and implication for blazar physics

Circular polarization is detected at the 3σ level in two HPQs: 1256–229 and 2155–152 (Table 2). On April 21, we had the opportunity to re-measure the linear polarization of these objects in the V filter, after replacing the quarter-wave plate by the half-wave plate (HWP) (cf. Saviane et al. 2007). Four exposures with the HWP rotated to 0° , 22.5° , 45° , and 67.5° were secured and reduced in the standard way (e.g. Sluse et al. 2005). The results are reported in Table 4, together with the circular polarization measurements from Table 2. Although the optical linear polarization of these quasars is high, the circular polarization we measured at the same epoch is above the 3σ upper limit on the circular polarization generated by the instrumental cross-talk (Sect. 2).

In Table 4, we also summarize the main polarization properties of these objects, including measurements at radio wavelengths. For completeness, we include the BL Lac object for which circular polarization was found to be significant after averaging the UBVRI measurements (Table 3). As far as we know, these are the only 3σ detections of optical circular polarization in quasars, in addition to those reported by Wagner & Mannheim (2001) for 3C279¹ (= 1253–055). Although variable (as commonly seen in HPQs), the optical linear polarization is high in

Table 4. Radio to optical polarization characteristics of objects with detected optical circular polarization.

1256–229 (PKS) $z = 0.481$				HPQ, BL Lac?
Date	ν (Ghz)	p_{lin} (%)	θ_{lin} ($^{\circ}$)	p_{circ} (%)
03/2002	5.4×10^5	22.32 ± 0.15	157 ± 1^d	–
04/2007	5.4×10^5	15.42 ± 0.16	163 ± 1^j	0.18 ± 0.04^j
2155–152 (PKS) $z = 0.672$				HPQ
Date	ν (Ghz)	p_{lin} (%)	θ_{lin} ($^{\circ}$)	p_{circ} (%)
08/1984	5.4×10^5	32.70 ± 1.30	6 ± 1^a	–
04/2007	5.4×10^5	17.67 ± 0.49	51 ± 1^j	-0.35 ± 0.10^j
09/2007	85.6	11.04 ± 0.53	52 ± 1^i	$<0.93^i$
03/2003	15.4	3.66	– ^f	$<0.34^f$
1979–1999	8.0	4.81 (mean)	– ^h	–
		15.3 (max)	– ^h	–
0219+428 (3C66A) $z = 0.444$				BL Lac
Date	ν (Ghz)	p_{lin} (%)	θ_{lin} ($^{\circ}$)	p_{circ} (%)
01/1992	5×10^5 [w]	31.07 ± 0.31	39 ± 1^b	0.76 ± 0.10^b
12/1999	5×10^5 [w]	26.11 ± 0.19	3 ± 1^c	0.16 ± 0.05^c
11/2008	85.6	4.36 ± 0.54	3 ± 4^i	$<0.73^i$
12/1996	5.0	2.9	– ^e	$<0.20^e$
1974–1999	8.0	2.96 (mean)	– ^g	–

Notes. Multi-color measurements in references (b) and (c) were averaged; upper limits are given at 3σ . References for linear or circular polarization: ^(a) Brindle et al. (1986); ^(b) Takalo & Sillanpää (1993); ^(c) Tommasi et al. (2001b); ^(d) Sluse et al. (2005); ^(e) Homan et al. (2001); ^(f) Homan & Lister (2006); ^(g) Fan et al. (2006); ^(h) Fan et al. (2008); ⁽ⁱ⁾ Agudo et al. (2010); ^(j) this work.

all three objects suggesting that a relation exists between linear and circular polarization.

Radio circular polarization has been detected in a small number of blazars with typical values of a few tenths of a percent (Weiler & de Pater 1983; Rayner et al. 2000; Homan et al. 2001; Homan & Lister 2006; Vistrishchak et al. 2008). Although the origin of the radio circular polarization is not yet understood, two main mechanisms of production have been proposed: intrinsic circular polarization of the relativistically beamed synchrotron radiation (which also produces the radio linear polarization) and Faraday conversion of linear to circular polarization (e.g. Wardle & Homan 2003). Since beamed synchrotron radiation can also explain the high optical linear polarization observed in HPQs and contribute significantly to the optical continuum (Impey & Tapia 1990; Wills et al. 1992), a similar origin to both the optical and the radio circular polarizations appears likely although they most probably arise from different regions. Since Faraday conversion is inefficient at visible wavelengths, the detected optical circular polarization should be caused by synchrotron emission. Since intrinsic circular polarization is not produced in a positron-electron plasma, this mechanism requires the predominance of a proton-electron plasma, as already suggested by circular polarization measurements obtained at millimeter wavelengths (Agudo et al. 2010). Furthermore, if circular polarization is intrinsic, a correlation between the linear and the circular polarization degrees is expected, the high recorded values indicating a rather homogeneous magnetic field whose strength should be of the order of 1 kG (e.g. Valtaoja et al. 1993). This is much higher than usually assumed in quasar jets, and can only occur in small regions close to the quasar core (Wardle & Homan 2003; Silant'ev et al. 2009; Piotrovich et al. 2010). On

¹ Wagner et al. (2000) reported that $p_{\text{circ}} = 0.25 \pm 0.03\%$, while Wagner & Mannheim (2001) reported $p_{\text{circ}} = 0.45 \pm 0.03\%$. These detections

were considered tentative by the authors in view of significant instrumental effects and thus not included in Tables 3 and 4.

the other hand, the optical continuum could predominantly arise from inverse Compton scattering of radio synchrotron radiation, a mechanism that preserves the circular polarization (Sciama & Rees 1967). This would require a significant circular polarization at radio wavelengths, which is apparently not observed (Table 4). Given the uncertainties and the non-simultaneous observations, no firm conclusion can be derived. Unveiling the origin of the optical circular polarization – even a few tenths of a percent – thus appears challenging (see also Rieger & Mannheim 2005). A clearer understanding would require simultaneous observations at radio and optical wavelengths.

4. Conclusions

We have reported new accurate measurements of optical circular polarization in the V filter for a sample of 21 quasars. For most objects, the uncertainties are smaller than 0.1%, and smaller than 0.05% for six of them.

All objects have null polarization within the uncertainties except two highly linearly polarized blazars. This has allowed us to constrain the polarization caused by photon-pseudoscalar mixing along the line of sight, ruling out the interpretation of the observed alignments of quasar polarization vectors in terms of photon-pseudoscalar mixing, at least in the framework of a simple formulation.

We also found small but significant optical circular polarization in two blazars, providing clues about the strength of the magnetic fields, the nature of the jets and/or the dominant emission mechanism. Our observations demonstrate that optical circular polarization is routinely measurable with present day high-accuracy polarimeters.

Acknowledgements. D.H. thanks Alexandre Payez and Jean-René Cudell for useful discussions. A fellowship from the Alexander von Humboldt Foundation to D.S. is gratefully acknowledged. This research has made use of data originally from the University of Michigan Radio Astronomy Observatory, which has been supported by the University of Michigan and the National Science Foundation.

References

Agudo, I., Thum, C., Wiesemeyer, H., & Krichbaum, T. P. 2010, *ApJS*, 189, 1
 Berriman, G., Schmidt, G. D., West, S. C., & Stockman, H. S. 1990, *ApJS*, 74, 869
 Brindle, C., Hough, J. H., Bailey, J. A., Axon, D. J., & Hyland, A. R. 1986, *MNRAS*, 221, 739
 Collinge, M. J., Strauss, M. A., Hall, P. B., et al. 2005, *AJ*, 129, 2542
 Das, S., Jain, P., Ralston, J. P., & Saha, R. 2005, *JCAP*, 06, 002
 Fan, J.-H., Hua, T.-X., Yuan, Y.-H., et al. 2006, *PASJ*, 58, 94
 Fan, J.-H., Yuan, Y.-H., Hua, T.-X., et al. 2008, *PASJ*, 60, 707
 Gnedin, Y. N., Piotrovich, M. Y., & Natsvlishvili, T. M. 2007, *MNRAS*, 374, 276
 Fossati, L., Bagnulo, S., Mason, E., & Landi Degl’Innocenti, E. 2007, *ASPC* 364, 503
 Homan, D. C., Attridge, J. M., & Wardle, J. F. C. 2001, *ApJ*, 556, 113
 Homan, D. C., & Lister, M. L. 2006, *AJ*, 131, 1262
 Hutsemékers, D. 1998, *A&A*, 332, 410
 Hutsemékers, D., & Lamy, H. 2001, *A&A*, 367, 381
 Hutsemékers, D., Lamy, H., & Remy, M. 1998, *A&A*, 340, 371
 Hutsemékers, D., Cabanac, R., Lamy, H., & Sluse, D. 2005, *A&A*, 441, 915
 Hutsemékers, D., Payez, A., Cabanac, R., et al. 2008, in *Astronomical Polarimetry 2008: Science from Small to Large Telescopes*, ed. P. Bastien and N. Manset, *ASP Conf. Ser.*, in press [[arXiv:0809.3088](https://arxiv.org/abs/0809.3088)]
 Impey, C. D., & Tapia, S. 1990, *ApJ*, 354, 124
 Impey, C. D., Malkan, M. A., Webb, W., & Petry, C. E. 1995, *ApJ*, 440, 80
 Jain, P., Panda, S., & Sarala, S. 2002, *Phys. Rev. D*, 66, 085007
 Jordan, S., & Friedrich, S. 2002, *A&A*, 383, 519
 Lamy, H., & Hutsemékers, D. 1999, *The Messenger*, 96, 25
 Lamy, H., & Hutsemékers, D. 2000, *A&AS*, 142, 451
 Landstreet, J. D., & Angel, J. R. P. 1972, *ApJ* 174, L127
 Moore, R. L., & Stockman, H. S. 1981, *ApJ*, 243, 60
 Moore, R. L., & Stockman, H. S. 1984, *ApJ*, 279, 465
 Payez, A., Cudell, J. R., & Hutsemékers, D. 2008, *AIP Conf. Proc.*, 1038, 211
 Payez, A., Cudell, J. R., & Hutsemékers, D. 2010a, *Proc. of the 5th Patras Workshop on Axions, WIMPs and WISPs, DESY-PROC-2009-5*, 133
 Payez, A., Cudell, J. R., & Hutsemékers, D. 2010b, *AIP Conf. Proc.*, 1241, 444
 Piotrovich, M. Y., Gnedin, Y. N., Natsvlishvili, T. M., & Silant’ev, N. A. 2010, *Astron. Lett.*, 36, 389
 Raffelt, G., & Stodolsky, L. 1988, *Phys. Rev. D*, 37, 1237
 Rayner, D. P., Norris, R. P., & Sault, R. J. 2000, *MNRAS*, 319, 484
 Rieger, F. K., & Mannheim, K. 2005, *Chin. J. Astron. Astrophys.*, 5, 311
 Saviane, I., Piirola, V., Bagnulo, S., et al. 2007, *The Messenger*, 129, 14
 Sbarufatti, B., Treves, A., Falomo, R., et al. 2005, *AJ*, 129, 559
 Scarpa, R., & Falomo, R. 1997, *A&A*, 325, 109
 Sciama, D. W., & Rees, M. J. 1967, *Nature*, 216, 147
 Schmidt, G. D., & Hines, D. C. 1999, *ApJ*, 512, 125
 Silant’ev, N. A., Piotrovich, M. Y., Gnedin, Y. N., & Natsvlishvili, T. M. 2009, *A&A*, 507, 171
 Sluse, D., Hutsemékers, D., Lamy, H., Cabanac, R., & Quintana, H. 2005, *A&A*, 433, 757
 Stockman, H. S., Moore, R. L., & Angel, J. R. P. 1984, *ApJ*, 279, 485
 Takalo, L. O., & Sillanpää, A. 1993, *Ap&SS*, 206, 191
 Tommasi, L., Diaz, R., Pallazzi, E., et al. 2001a, *ApJS*, 132, 73
 Tommasi, L., Palazzi, E., Pian, E., et al. 2001b, *A&A*, 376, 51
 Turnshek, D. A., Bohlin, R. C., Williamson, R. L., et al. 1990, *AJ*, 99, 1243
 Valtaoja, L., Karttunen, H., Valtaoja, E., Shakhovskoy, N. M., & Efimov, Y. S. 1993, *A&A*, 273, 393
 Véron-Cetty, M.-P., & Véron, P. 2006, *A&A*, 455, 773
 Vitrischchak, V. M., Gabuzda, D. C., Algaba, J. C., et al. 2008, *MNRAS*, 391, 124
 Visvanathan, N., & Wills, B. J. 1998, *AJ*, 116, 2119
 Wagner, S. J., & Mannheim, K. 2001, *ASPC*, 250, 142
 Wagner, S. J., Seifert, W., Appenzeller, I., et al. 2000, *Proc. SPIE*, 4005, 95
 Wardle, J. F. C., & Homan, D. C. 2003, *Ap&SS*, 288, 143
 Weiler, K. W., & de Pater, I. 1983, *ApJS*, 52, 293
 West, S. C. 1989, *ApJ*, 345, 511
 Wills, B. J., Wills, D., Breger, M., Antonucci, R. R. J., & Barvainis, R. 1992, *ApJ*, 398, 454

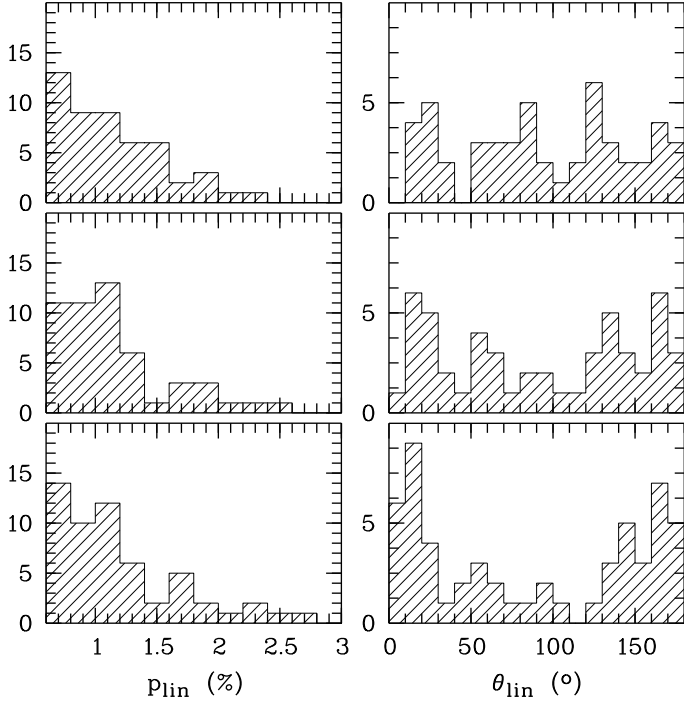


Fig. A.1. The effect of the addition of a small systematic polarization Δp_{lin} on the distributions of the polarization degree p_{lin} and of the polarization angle θ_{lin} . From top to bottom, $\Delta p_{\text{lin}} = 0\%$, 0.25% , and 0.5% (see text for details).

Appendix A: The determination of Δp_{lin}

Although partly discussed in previous papers (e.g. Hutsemékers et al. 2005), we provide some details of the simulations performed to estimate Δp_{lin} , the small additional linear polarization needed to reproduce the observed alignments of quasar polarization vectors. These simulations extend those discussed in Hutsemékers & Lamy (2001), accounting for the measurement errors.

We first modeled the distribution of the debiased polarization degree in the full quasar sample (from Hutsemékers et al. 2005, including objects with $p < 0.6\%$). We found that it was reasonably well reproduced by a half-gaussian distribution of zero mean and unitary variance. According to this distribution, we randomly generate 80 values of the polarization degree p , most of them lying between 0% and 3%. We also generate 80 values of the polarization angle θ , uniformly distributed between 0° and 180° . From p and θ , we compute the normalized Stokes parameters q and u to which we add a systematic polarization $\Delta q > 0$ (we assume for simplicity that $\Delta u = 0$, which corresponds to add linear polarization at $\theta = 0^\circ$). We also add random noise uniformly generated between -0.2% and $+0.2\%$, in agreement with the uncertainties in the measurements (Hutsemékers et al. 2005). Finally, from the modified q and u we recompute p , θ , and σ_θ in the usual way and select the good quality measurements with the criteria previously used, i.e., $p \geq 0.6\%$ and $\sigma_\theta \leq 14^\circ$. This leaves us with ~ 60 polarization values. This is comparable to the number of objects in the alignment region (cf. Fig. 7 of Hutsemékers et al. 2005, to which these simulations should be compared).

The results are illustrated in Fig. A.1 for $\Delta q = 0\%$, 0.25% , and 0.5% from top to bottom. We see that, in the distribution of

polarization angles, a significant deviation to uniformity is only obtained for $\Delta p_{\text{lin}} = \Delta q = 0.5\%$. At the same time, the distribution of the polarization degree does not appear significantly modified. Since this additional polarization at a single polarization angle is likely unrealistic, Δp_{lin} should be seen as a lower limit, although it cannot be much higher. Indeed, much larger values would make the distribution of the polarization degree incompatible with the observations (e.g. Hutsemékers & Lamy 2001).

Appendix B: Circular polarization due to photon-pseudoscalar mixing

In the weak mixing case, photons with polarizations parallel to an external magnetic field \mathbf{B} that propagate through the distance L can decay into pseudoscalars with a probability

$$P_{\gamma a} \simeq (gBl)^2 \sin^2(\xi/2), \quad (\text{B.1})$$

where $l = 2\omega/(\omega_p^2 - m_a^2)$ and $\xi = L/l$, ω is the photon frequency, ω_p the plasma frequency, m_a the pseudoscalar mass, and g the photon-pseudoscalar coupling constant (Raffelt & Stodolky 1988; Jain et al. 2002). As long as $P_{\gamma a}$ is small, the linear polarization perpendicular to \mathbf{B} generated by dichroism can be approximated by $\Delta p_{\text{lin}} = P_{\gamma a}$. The mixing also induces a polarization-dependent phase shift (retardance)

$$\phi_a \simeq \left(\frac{gBl}{2} \right)^2 (\xi - \sin \xi) \quad (\text{B.2})$$

acquired by the photons during propagation, which results in circular polarization. As noted by Raffelt & Stodolky (1988), both effects are on the order of $(gBl)^2$.

Assuming $m_a \ll \omega_p$, we have $l \simeq 4 \times 10^{-14} \nu n_e^{-1} \text{ Mpc}$, where ν is the frequency in GHz and n_e the electronic density in cm^{-3} . At optical wavelengths ($\nu = 5 \times 10^5$ GHz) and under various conditions (e.g. $n_e \sim 10^{-6} \text{ cm}^{-3}$ and $L \sim 10 \text{ Mpc}$ in superclusters, or $n_e \sim 10^{-8} \text{ cm}^{-3}$ and $L \sim 1 \text{ Gpc}$ in the intergalactic medium), $\xi = L/l \sim 500$. With a frequency bandwidth $\Delta\nu/\nu \sim 0.2$ and $\xi \gg 1$, we find that $\phi_a \simeq \langle \Delta p_{\text{lin}} \rangle \xi/2 \sim 10^2 \langle \Delta p_{\text{lin}} \rangle$, where $\langle \Delta p_{\text{lin}} \rangle$ represents the average value of Δp_{lin} . Similar estimates are derived when accounting for density fluctuations (Jain et al. 2002).

Adopting the convention of $u = 0$ and $q > 0$ for polarization vectors parallel to \mathbf{B} , the dichroism and birefringence induced by photon-pseudoscalar mixing modify the polarization according to

$$\begin{aligned} q &= q_0 - \Delta p_{\text{lin}}, \\ u &= u_0 \cos \phi_a, \\ v &= u_0 \sin \phi_a, \end{aligned} \quad (\text{B.3})$$

where q_0 and u_0 are the normalized Stokes parameters representing the initial linear polarization state and $v_0 = 0$. Assuming that the sources are initially polarized at $p_0 \simeq 2\%$ with randomly oriented polarization angles and that $\langle \Delta p_{\text{lin}} \rangle < 0.01$ (Appendix A), we finally obtain the average circular polarization expected to result from the photon-pseudoscalar mixing: $\langle |v| \rangle \sim (2/\pi)p_0 \phi_a$, i.e., $\langle |p_{\text{circ}}| \rangle \sim \langle \Delta p_{\text{lin}} \rangle \sim 0.5\%$. This estimate applies to a variety of plausible situations, in agreement with the simulations shown in Das et al. (2005), Hutsemékers et al. (2008), and Payez et al. (2008).